Fermi surface and interlayer transport in the two-dimensional magnetic organic conductor (Me-3,5-DIP)[Ni(dmit)$_2$]$_2$

K. Hazama and S. Uji
Graduate School of Pure and Applied Sciences, University of Tsukuba, Tsukuba, Ibaraki 305-8577, Japan
and National Institute for Materials Science, Tsukuba, Ibaraki 305-0003, Japan

Y. Takahide, M. Kimata, H. Satsukawa, A. Harada, and T. Terashima
National Institute for Materials Science, Tsukuba, Ibaraki 305-0003, Japan

Y. Kosaka, H. M. Yamamoto, and R. Kato
RIKEN, Wako, Saitama 351-0198, Japan

(Received 29 July 2010; revised manuscript received 25 March 2011; published 29 April 2011)

Resistance and magnetic torque measurements at low temperatures under high magnetic fields have been performed for a magnetic organic conductor (Me-3,5-DIP)[Ni(dmit)$_2$]$_2$ to investigate the electronic state. This conductor contains two types of Ni(dmit)$_2$]$_2$ anion layers, layers I and II. Shubnikov-de Haas and angular-dependent magnetoresistance oscillations clearly show that there exists a two-dimensional Fermi surface in layer II, whose spins are strongly coupled with the localized spins in layer I. When the magnetic field is applied parallel to the layers, the interlayer resistance shows a sharp minimum at ∼8 T and then slow oscillation at higher fields. The minimum is explained by the combined effect of the field-dependent magnetic potential and momentum shift in the interlayer tunneling. The mechanism of the slow oscillation is not clarified yet.

DOI: 10.1103/PhysRevB.83.165129 PACS number(s): 71.18.+y, 71.20.Rv, 72.15.Gd

I. INTRODUCTION

Variousorganic conductors containing magnetic moments have been extensively studied because the coexistence of conduction electrons and localized spins has lead to many intriguing phenomena.[1–3] One of the best examples is magnetic-field-induced superconductivity found in λ-(BETS)$_2$FeCl$_4$,[4–6] where the superconductivity is stabilized only in high magnetic fields. In this field-induced superconductivity, a crucial rule is played by the so-called π-d interaction, superexchange interaction between the conduction π electrons in the BETS cation layers, and the localized 3d moments in the $FeCl_4$ anions ($S = 5/2$). In the past decades, various magnetic organic conductors have been synthesized.[7–14] For most of them, there exist localized $3d$ moments in the insulating anion layers between the donor molecule layers.

An organic conductor (Me-3,5-DIP)[Ni(dmit)$_2$]$_2$,[15] where Me = methyl, DIP = diiodopyridinium, and dmit = 1,3-dithiol-2-thione-4,5-dithiolate, includes no d moments, but has both localized and itinerant π electrons in the organic molecule layers. The crystal structure of (Me-3,5-DIP)[Ni(dmit)$_2$]$_2$ [Fig. 1(a)] has monoclinic symmetry; $C2/c$, $a = 14.3480(6)$, $b = 6.4710(3)$, $c = 76.556(3)$ Å, $\beta = 92.989(3)^\circ$, $V = 7098.2(5)$ Å^3, and $Z = 8$. The unit cell contains two types of Ni(dmit)$_2$ anion layers, layers I and II, which are crystallographically independent.

In layer I, the band-structure calculation based on a tight-binding approximation shows the presence of an extremely narrow band, whose width is much smaller than the effective on-site Coulomb interaction. Therefore, the electronic state in layer I is expected to be a Mott insulating state. On the other hand, in layer II, the Ni(dmit)$_2$ anions have two large transfer integrals between the neighboring molecules. This structure gives a much wider energy band, stabilizing a metallic state. The band-structure calculation predicts the presence of a two-dimensional (2D) Fermi surface with an elliptical cross section as shown in Fig. 1(b).

The resistivity along the crystal a or b axis shows essentially metallic behavior down to the lowest temperature.[15] The resistivity along the c axis is four orders of magnitude larger than that along the a or b axis. The large anisotropy shows the presence of a highly 2D electronic state as predicted from the band-structure calculation. The magnetic susceptibility increases with decreasing temperature, has a maximum at ∼20 K, and then decreases. The temperature dependence above 40 K can be fitted by a Curie-Weiss term [$\chi_{CW} = C/(T-\theta), C = 0.375$ emu K mol^{-1}, $\theta = -5$ K] and constant term ($\chi_{const} = 7.2 \times 10^{-4}$ emu mol^{-1}). The Curie-Weiss term of the susceptibility shows that there exist localized π spins, which are antiferromagnetically coupled with each other. From the band-structure calculation, the localized spins are assigned to those in layer I. The constant term of the susceptibility can be ascribed to the Pauli paramagnetism of the conduction electrons in layer II. The large paramagnetism and the high conductivity should arise solely from the Ni(dmit)$_2$ layers because the Me-3,5-DIP cations are closed-shell molecules. Recent ^{13}C NMR measurements reveal the presence of both the insulating and metallic Ni(dmit)$_2$ layers. The NMR spectra also show an antiferromagnetic order or strong antiferromagnetic fluctuation of the localized spins at low temperatures.[16]

Due to the unique structure of (Me-3,5-DIP)[Ni(dmit)$_2$]$_2$, we could expect some different physical phenomena arising from the interaction between the localized- and itinerant-π electrons, if it is sufficiently large. To further investigate the electronic state of (Me-3,5-DIP)[Ni(dmit)$_2$]$_2$, we have systematically measured the quantum oscillations and angular-dependent magnetoresistance oscillations (AMROs). We have

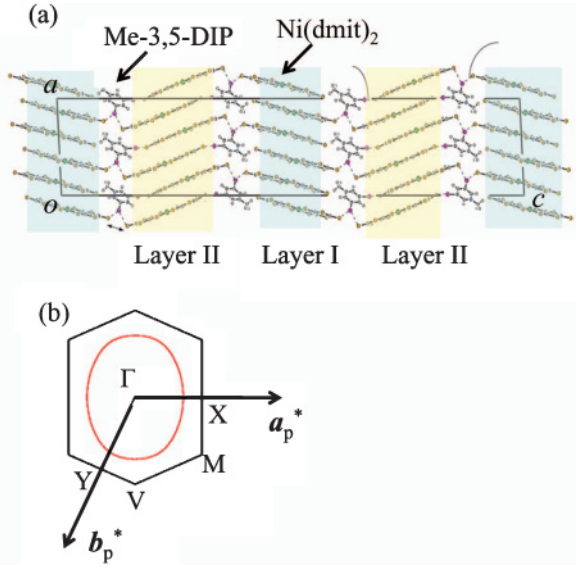

FIG. 1. (Color online) (a) Crystal structure of (Me-3,5-DIP)[Ni (dmit)$_2$]$_2$. (b) The first Brillouin zone and the Fermi surface in layer II obtained by the band-structure calculation. $\boldsymbol{a}_p^*$ and $\boldsymbol{b}_p^*$ show the reciprocal lattice vectors of the primitive cell. The unit vectors of the primitive cell are taken as $\boldsymbol{a}_p = (\boldsymbol{a} + \boldsymbol{b})/2$ and $\boldsymbol{b}_p = \boldsymbol{b}$ (from Ref. 14).

also performed magnetic torque measurements to examine the magnetic properties.

II. EXPERIMENT

Single crystals of (Me-3,5-DIP)[Ni(dmit)$_2$]$_2$ are synthesized electrochemically.[15] The crystals are platelike, whose basal planes are the *ab* planes. Two pairs of the electric contacts are made on the basal planes by a carbon paste and the resistance perpendicular to the layers is measured by a conventional ac four-probe method. The magnetic torque is measured by using a piezoresistive microcantilever.[17] The measurements are performed by a ^{4}He cryostat with a 17-T superconducting magnet, a dilution refrigerator with a 20-T superconducting magnet, or a ^{3}He cryostat with a 30-T resistive magnet at Tsukuba Magnet Laboratories.

III. RESULTS

A. Resistance

Figure 2 shows the temperature dependence of the *c*-axis (interlayer) resistance under magnetic fields. The field is applied parallel to the c^* axis, perpendicular to both *a* and *b* axes. At zero field, the resistance increases with decreasing temperature, has a maximum at ~80 K, and then decreases. As the temperature further decreases, an upturn is seen at ~25 K. The overall feature is consistent with the previous report.[15] No appreciable magnetoresistance is observed above 40 K. Below 40 K, however, we observe large negative magnetoresistance and the upturn at ~25 K at zero field is completely suppressed by field.

Recent x-ray diffraction measurements reveal that superlattice spots with fourfold periodicity gradually appear below 170 K and the periodicity changes to threefold below 110 K.[18]

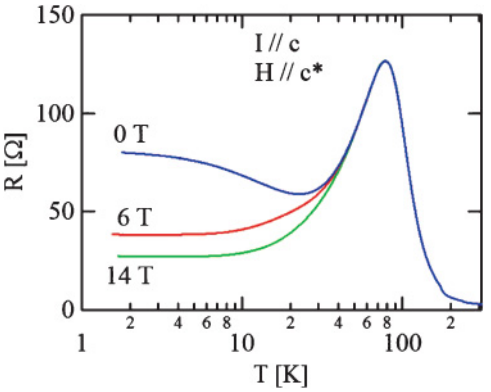

FIG. 2. (Color online) Temperature dependence of the *c*-axis resistance under magnetic fields for $H \parallel c^*$, perpendicular to both *a* and *b* axes.

At present, the origin is not clarified yet. Since the resistivity and the magnetic susceptibility do not exhibit any obvious anomalies at these temperatures, the electronic states are not strongly affected by the structural changes.

Figures 3(a) and 3(b) show the resistance as a function of the field angle θ at 1.8 K. The magnetic field angles are defined in the inset. Below 4 T, the resistance has a minimum for $\theta \approx 0°$, and broad maxima for $\theta \approx \pm 90°$. As the field increases, the maxima for $\theta \approx \pm 90°$ are suppressed and minima appear above 8 T. As the field further increases, maxima appear again for $\theta \approx \pm 90°$. In addition to this behavior, successive small peaks are observable above 8 T. As the field increases, the peaks for $|\theta| \lesssim 60°$ become more prominent although the peak positions do not shift. The results show that the oscillation is not caused by the quantum oscillation, but by AMRO.[19–22] The small peaks for $|\theta| \gtrsim 60°$ seem field dependent, whose origin is not clear.

To see the AMRO for $|\theta| \lesssim 60°$ more clearly, we plotted the second derivative curves of the resistance at various angles [Fig. 4(a)]. Most of the peaks are almost periodic as a function of tan θ, but the peaks close to $\theta = 0$ (denoted by arrows) are isolated from the others. The origin of the isolated peaks is not clear at present. The AMRO is asymmetric around $\theta = 0$. The main reason is probably the monoclinic symmetry of the crystal structure. A similar asymmetric AMRO is reported in (BEDT-TTF)$_2$Br(DIA) with a triclinic symmetry.[23]

When a 2D Fermi surface is assumed, the period δ of the AMRO is given by $\delta(\phi) = \pi/dk_\parallel(\phi)$, where $k_\parallel$ is the projection of the Fermi wave number $k_F(\phi)$ on the conduction plane. The relation between $k_\parallel$ and k_F is given by[21,22,24]

$$k_\parallel(\phi)^2 = \left[k_{\mathrm{F}}^{\mathrm{short}}\cos(\phi - \xi)\right]^2 + \left[k_{\mathrm{F}}^{\mathrm{long}}\sin(\phi - \xi)\right]^2, \quad (1)$$

where $k_{\mathrm{F}}^{\mathrm{short}}$ ($k_{\mathrm{F}}^{\mathrm{long}}$) is the shortest (longest) Fermi wave number of the elliptic cross section, and ξ is the inclination angle of the major axis. From the AMRO measurements for various ϕ, we can make the polar plot of $k_\parallel$ in Fig. 4(b), assuming that one of the two layers has a 2D Fermi surface; $d = c/2\sin(\beta)$. The ellipsoid in Fig. 4(b) shows the cross section of the 2D Fermi surface obtained from $k_{\mathrm{F}}^{\mathrm{short}} = 0.34$ Å^{-1} and $k_{\mathrm{F}}^{\mathrm{long}} = 0.45$ Å^{-1}. The cross section corresponds to ~57% of the first Brillouin zone (BZ), which is somewhat bigger than 50%

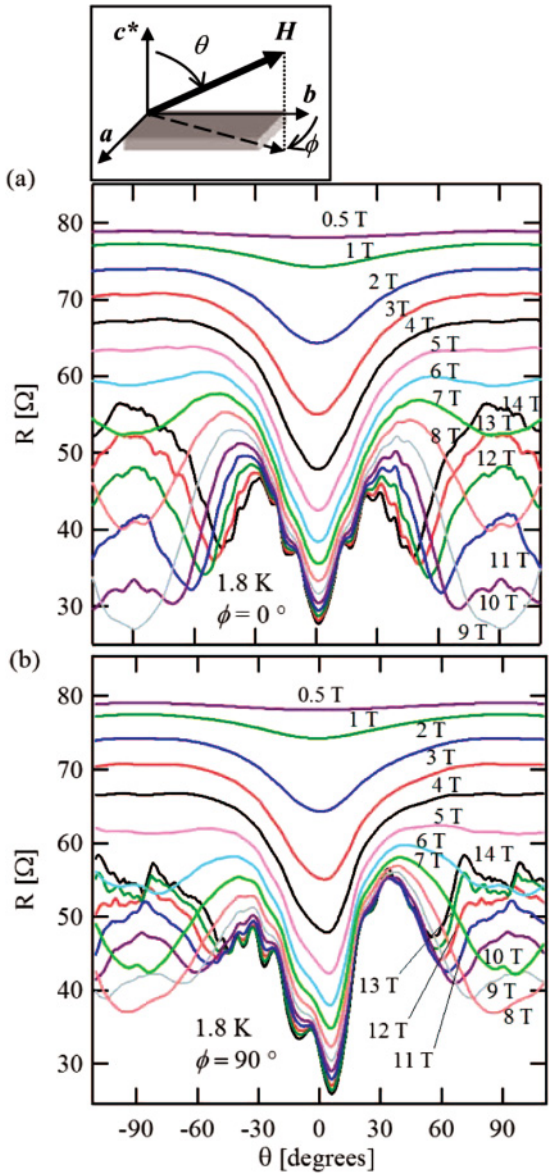

FIG. 3. (Color online) AMRO measurements at various fields for (a) $\phi = 0^\circ$ and (b) $\phi = 90^\circ$ Inset: Definition of the magnetic field angles θ and ϕ.

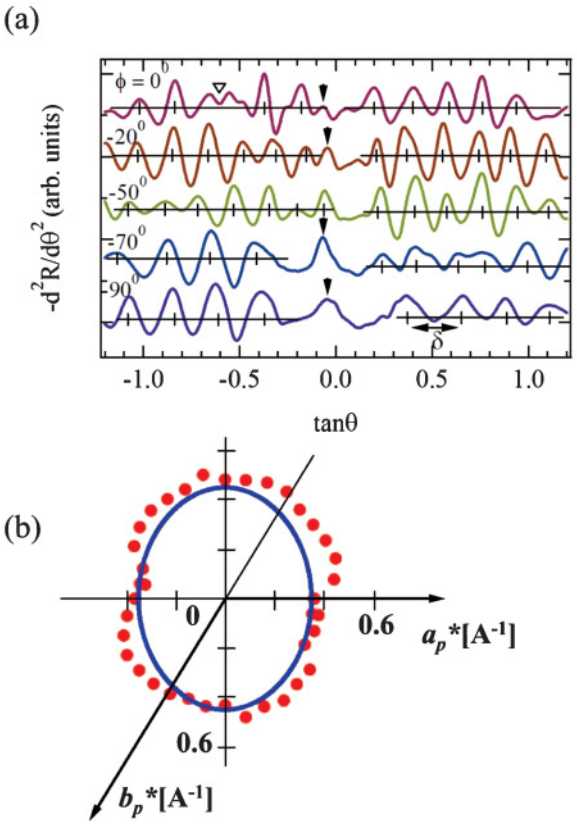

FIG. 4. (Color online) (a) The second derivative curves of the AMRO data at 14 T. Peaks isolated from the periodic ones are denoted by arrows. The triangle for $\phi = 0$ indicates a missing peak for some reason. (b) Polar plot of $k_\parallel$. The ellipsoid (solid curve) shows the cross section of the 2D Fermi surface.

expected from the band-structure calculation. This discrepancy is probably within the experimental error because the δ values are somewhat scattered.

The AMRO observed in 2D systems has been interpreted in the framework of the Boltzmann transport theory,[19–22] where the semiclassical trajectories of the electrons on the corrugated 2D Fermi surface (coherent interlayer transport) are taken into account. Fully quantum mechanical treatment reveals that the same AMRO appears even when the interlayer transport is weakly incoherent;[25–27] the carriers are scattered in the layers more frequently than the tunneling rate between the layers. In this case, the 2D Fermi surface without energy dispersion along the interlayer direction is defined in each layer. One of the decisive tests for the coherent interlayer transport is the observation of a sharp interlayer resistance peak under sufficiently high fields parallel to the layers. This peak originates from the closed orbits formed at the sides of the corrugated Fermi surface.[28] We have carefully measured the resistance, but found no sharp resistance peak up to 14 T for $\theta \approx \pm 90^\circ$. The NMR measurements reveal the presence of both the insulating and metallic Ni(dmit)$_2$ layers.[16] Because of the stacking structure, the magnetic insulating layer is recognized as a tunnel barrier for the interlayer transport as discussed later. Therefore, it is likely that the interlayer transport is within a weakly incoherent regime, although the absence of the sharp peak for $\theta \approx \pm 90^\circ$ is not definitive evidence.

Figure 5 shows the resistance as a function of magnetic field perpendicular to the conducting layer at 26 mK. With increasing field, the resistance first decreases and has a tendency to saturate above 10 T. Above 8 T, we see the Shubnikov-de Hass (SdH) oscillation with some nodes. The insets show a closeup of the SdH oscillation at ~15 T and the Fourier transform (FT) spectrum of the oscillation. In the FT spectrum, we see two peaks with slightly different frequencies F_1 and F_2. The average frequency $F = (F_1 + F_2)/2 = 4577$ (T) gives the cross section of 51.6% to the first BZ. This value well agrees with the structure calculation. From the temperature dependence, we obtain the effective mass $m_{\rm eff}$ of $6m_0$, where m_0 is the free electron mass. No meaningful difference of the effective masses is found between the two oscillations F_1 and F_2. The Dingle temperature of 0.6 K is obtained from the field dependence of the oscillation.

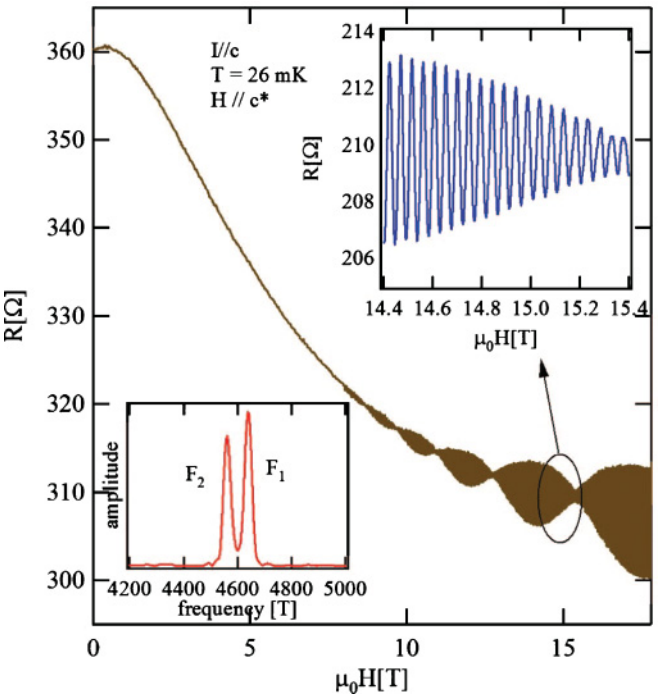

FIG. 5. (Color online) The resistance in magnetic field perpendicular to the conduction layers. Insets: Closeup of the SdH oscillation at ∼15 T and the Fourier transform spectrum of the oscillation between 8 and 18 T.

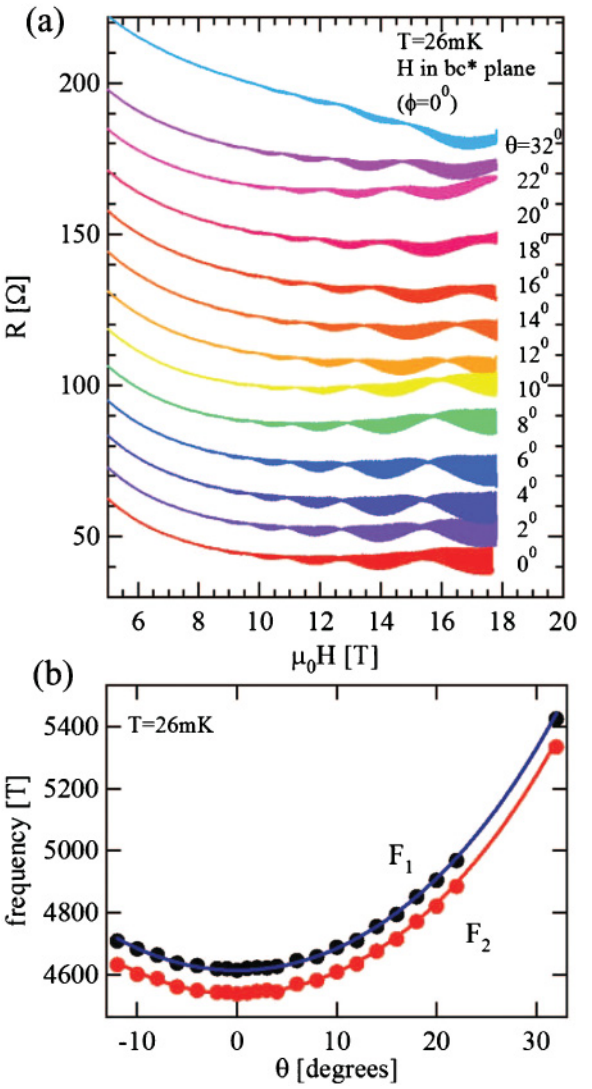

FIG. 6. (Color online) (a) The field dependence of the resistance at various angles. Each curve is shifted for clarity. (b) The magnetic field angle dependence of the SdH oscillation frequencies obtained from the SdH oscillations shown in (a). The solid lines show $1/\cos\theta$ dependences expected for the 2D Fermi surface.

Figure 6(a) presents the field dependence of the resistance at various angles for H in the bc^* plane. We note that all the curves show the SdH oscillations with nodes. Figure 6(b) presents the field angle dependence of the frequencies obtained from the FT spectra of the SdH oscillations shown in Fig. 6(a). Both frequencies completely follow $1/\cos\theta$ dependences in the whole angle region. When the two frequencies arise from two extremal (maximum and minimum) cross sections of a single corrugated 2D Fermi surface, they should coincide with each other at the AMRO peak angles ($\theta = 4.8°, 12.7°, 23.6°, \ldots$). No such behavior in Fig. 6 shows that there exist two different 2D Fermi surfaces without corrugation. The result is consistent with the absence of the resistance peaks for $\theta \approx \pm 90°$ (weakly incoherent transport picture). It is also consistent with the quite high anisotropy ($\sim 10^4$) between the in-layer and interlayer resistances. The NMR measurements reveal the presence of both the insulating and metallic $Ni(dmit)_2$ layers[16] and the band-structure calculation suggests that layer I is a Mott insulator.[15] Therefore, the two 2D Fermi surfaces will be formed in layer II.

Figure 7(a) shows the resistance as a function of magnetic field nearly parallel to the conducting layer at 26 mK. The resistance shows a sharp minimum at ∼8 T and then increases. Slow oscillation is observed above 10 T for $\theta > 70°$. The oscillation is periodic as a function of the inverse magnetic field [Fig. 7(b)], as conventional SdH oscillation. The $1/\cos\theta$ dependence of the frequency [Fig. 7(c)] may suggest the presence of a small 2D Fermi surface. Assuming a 2D Fermi surface, we obtain the cross section of 0.36% to the first BZ. At present, since the observation of the low frequency is limited in the small angle range, we cannot exclude the possibility of a small 3D Fermi surface.

Very low frequencies unexpected from the band-structure calculations have been observed in some other organic conductors, θ-$(BEDT\text{-}TTF)_2I_3$,[29] α-$Et_2Me_2N[Ni(dmit)_2]_2$,[30] $(BEDT\text{-}TTF)_2Br(DIA)$,[23] and κ-$(BETS)_2FeBr_4$.[31,32] The origins of these small Fermi surfaces have been discussed in terms of the orbital of the counterions or lowest unoccupied molecular orbital (LUMO) in addition to highest occupied molecular orbital (HOMO) of the donor molecules, but no satisfactory interpretation has been given.

We performed interlayer resistance measurements up to 25 T for a different sample from the same batch (Fig. 8). The temperature dependence of the resistance for the sample is consistent with the data in Fig. 2. At 0.6 K, the resistance has a minimum at 9 T in fields parallel to the b axis ($\phi = 0°$ and $\theta = 90°$) and the minimum shifts to a high field as the field is

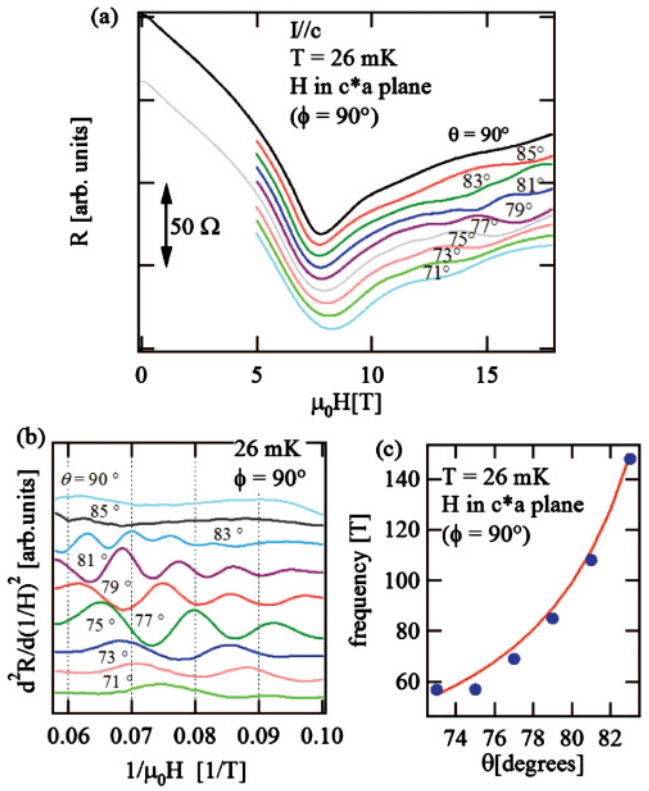

FIG. 7. (color online) (a) Resistance as a function of magnetic field. Each curve is shifted for clarity. (b) The second derivative curve of the resistance vs the inverse field. (c) The magnetic field angle dependence of the oscillation frequency. The solid line shows $16/\cos\theta$ (T).

tilted from the b axis to the c^* axis [Fig. 8(a)]. For $\theta < 30^\circ$, the minimum is not evident. The high- and low-frequency oscillations for $\theta < 30^\circ$ and $\theta > 50^\circ$ are consistent with the data in Figs. 5 and 7, respectively. The sharp minimum at 9 T is smeared out as the temperature increases and only monotonic positive magnetoresistance is observable for $T >$ 35 K [Fig. 8(b)].

B. Magnetic torque

Figures 9(a) and 9(b) show the magnetic torque curves as a function of the field angle at 26 mK. The torque τ is defined by $\tau = -\partial F/\partial\theta$, where F is the free energy of the electronic state. For a paramagnetic state, we may assume the magnetization, $M = M_1\cos^2(\theta') + M_2\sin^2(\theta')$, and then we obtain

$$\tau = \tfrac{1}{2}(M_1 - M_2)H\sin(2\theta'), \qquad (2)$$

where M_1 and M_2 are the magnetization along the principal axes, and θ' is the angle from the principal axis. We carefully measured the torque curves between 0.1 and 16 T, and found that all the torque curves are well reproduced by the above sine function. No appreciable anomalies arising from a spin-flip transition[33] is observed. Therefore, the localized spins remain paramagnetic (no long-range order) down to 26 mK. The minimum of the resistance at 8 T in Fig. 7(a) is not caused by any magnetic transitions, but by a crossover, as discussed later.

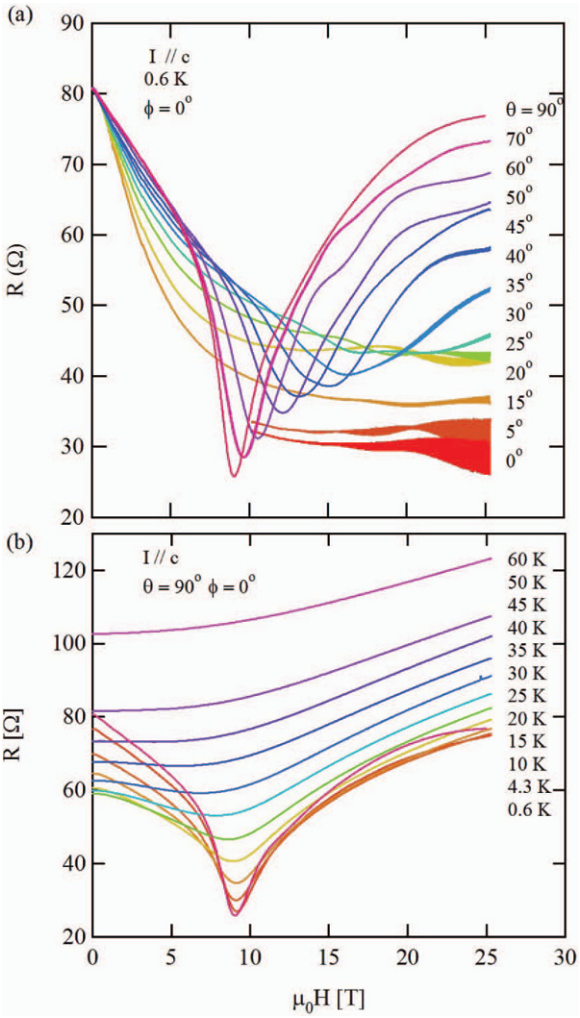

FIG. 8. (Color online) High-field interlayer resistance for a different sample from the same batch. (a) Resistance at various field angles. (b) Resistance at various temperatures.

Figure 10(a) shows the magnetic torque divided by field, corresponding to the anisotropy of the magnetization, $M_1(H) - M_2(H)$. In the whole field region, the curves show monotonic field dependence (no sign of a magnetic transition). Above 10 T, de Haas–van Alphen (dHvA) oscillations with some nodes are clearly observed [Fig. 10(b)]. The FT spectra [Fig. 10(c)] show double peaks, consistent with the SdH results. The torque-H curves tend to saturate at high fields but still change with field. Generally, the magnetization of localized spins (Curie-Weiss term) is much larger than that of conduction electrons (Pauli paramagnetism) at low temperatures. However, it is not necessarily the case for the torque measurements, because the torque is proportional to the magnetization anisotropy, not to the magnetization along the field. In the torque curves shown in Figs. 9 and 10, the contribution of the conduction π electrons, whose magnetization should be linear to H, is probably relatively large because the dHvA oscillations arising from the conduction π electrons are observed in high fields. It is likely that the magnetization of the localized spins is saturated at high fields, although we obtain no definitive evidence of the saturation from the torque measurements.

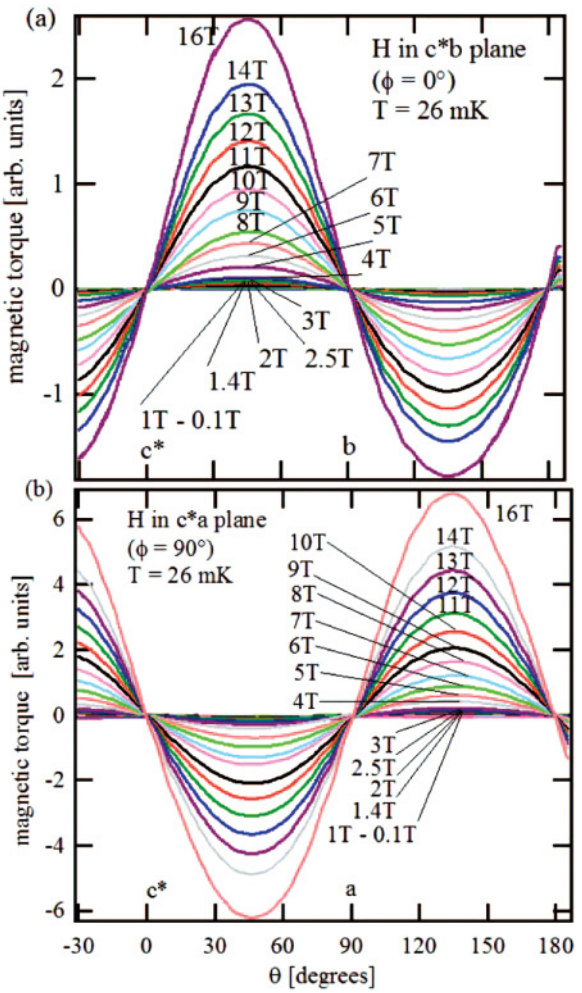

FIG. 9. (Color online) Magnetic torque as a function of the field angle θ at various magnetic fields for (a) H in the c^*b plane and (b) H in the c^*a plane.

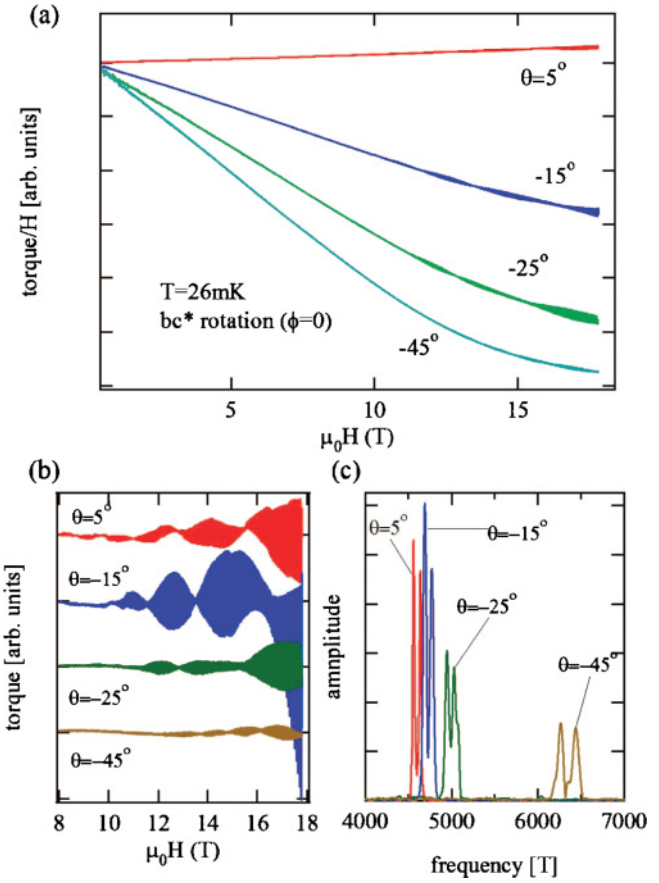

FIG. 10. (Color online) (a) Magnetic torque divided by field as a function of field. (b) Oscillatory part (dHvA oscillations) of the data shown in (a). (c) The FT spectra of the dHvA oscillations.

Figure 11 shows the peak-to-peak amplitude and the peak angle of the torque curve as a function of temperature. For both rotations, we note that the peak-to-peak amplitude increases with decreasing temperature, and has a broad maximum at ~20 K. For H in the c^*a plane, the upturn of the amplitude at 8 K is evident. The broad peak at 20 K is consistent with a maximum of the susceptibility.[15] The peak angle shows no significant temperature dependence. Since there exists no long-range order of the spins, the maximum of the amplitude at 20 K is ascribed to the short-range order, probably associated with strong antiferromagnetic fluctuation of the localized spins.[16]

IV. DISCUSSION

A. Internal magnetic field

We have obtained two important results in (Me-3,5-DIP)[Ni(dmit)$_2$]$_2$: (1) two 2D Fermi surfaces in layer II, and (2) the localized paramagnetic spins in layer I. First, we consider the interaction between the localized spins in layer I and the conduction electron spins in layer II. If they are coupled via exchange interaction J, the conduction electrons see internal field $H_{\rm int}$ created by the localized spins S, $H_{\rm int} = J\langle \boldsymbol{S}\rangle / g\mu_B$,

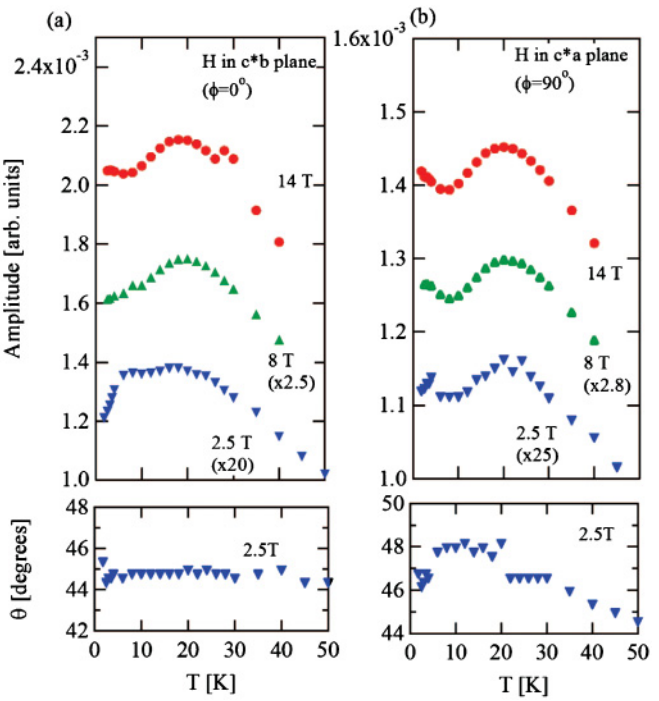

FIG. 11. (Color online) Peak-to-peak amplitude and the peak angle of the torque curve as a function of temperature for (a) H in the c^*b plane and (b) H in the c^*a plane.

where g and μ_B are the g factor and Bohr magneton, respectively. Assuming $H_{\rm int}$, we discuss the presence of two different frequencies of the quantum oscillations in detail below. In a strong magnetic field, the localized spins are likely polarized, $\langle \boldsymbol{S} \rangle \approx 1/2$; therefore, an almost fixed $H_{\rm int}$ may be given. Because of the Zeeman effect, the original energy band of the conduction electrons splits into the up- and down-spin bands. This means that two different 2D Fermi surfaces of the up and down spins are formed in magnetic field. In this case, the spin splitting factor $S_{\rm spin}$ in the Lifshitz-Kosevich formula is modified[34] and the resultant oscillatory term is given by

$$R_{\rm osc} \propto A_{\rm up} \cos\left[2\pi\left(\frac{F}{H}-\frac{1}{2}\right)-\pi S_{\rm spin}\right] + A_{\rm down}\cos\left[2\pi\left(\frac{F}{H}-\frac{1}{2}\right)+\pi S_{\rm spin}\right], \quad (3)$$

where F is the SdH frequency corresponding to the 2D Fermi surface. The prefactor A includes the temperature and Dingle reduction factors, which may be spin dependent. The modified spin splitting factor $S_{\rm spin}$ is

$$S_{\rm spin} = \frac{1}{2} g \frac{m_{\rm eff}}{m_0}\left(1-\frac{H_{\rm int}}{H}\right). \quad (4)$$

The internal field $H_{\rm int}$, proportional to the magnetization of the localized spins, may not be completely saturated even in the FT range between 10 and 18 T. However, it will be sufficient to take up to the first-order term of the Taylor expansion, $H_{\rm int} = H^0_{\rm int} + aH$. The small higher-order terms only broaden the FT peaks, which would not affect our conclusions. Substituting Eq. (4) into Eq. (3), we obtain

$$R_{\rm osc} \propto A_{\rm up} \cos\left[2\pi\left(\frac{F_1}{H}-\frac{1}{2}\right)-\pi S'_{\rm spin}\right] + A_{\rm down}\cos\left[2\pi\left(\frac{F_2}{H}-\frac{1}{2}\right)+\pi S'_{\rm spin}\right], \quad (5)$$

$$S'_{\rm spin} = \frac{1}{2} g \frac{m_{\rm eff}}{m_0}(1-a), \quad (6)$$

where $F_1 = F + \Delta F$ and $F_2 = F - \Delta F$. It should be noted that the first-order term aH modifies the phase of the oscillation, but not the frequency. The internal field $H^0_{\rm int}$ can be calculated from

$$\Delta F = \frac{1}{4} g \frac{m_{\rm eff}}{m_0} H^0_{\rm int}. \quad (7)$$

Substituting $g = 2$ and $m_{\rm eff} = 6m_0$, we obtain $\mu_0 H^0_{\rm int} \approx 13$ T from $\Delta F = 80$ T.

So far, large internal fields have been observed in π-d systems, λ-$(BETS)_2FeCl_4$ ($\mu_0 H_{\rm int} = 32$ T),[35,36] and κ-$(BETS)_2FeBr_4$ ($\mu_0 H_{\rm int} = 13$ T).[37,38] The internal field in (Me-3,5-DIP)$[Ni(dmit)_2]_2$ seems rather large in spite of the long distance between layers I and II. In (Me-3,5-DIP)$[Ni(dmit)_2]_2$, the band-structure calculation gives the interlayer transfer integral between layers I and II of $\sim$3 meV via the direct S-S coupling.[15] The value is much larger than those in BEDT-TTF based 2D organic conductors (usually almost zero). This is the reason why the conduction electron spins in layer II are strongly coupled with the localized spins in layer I. The Zeeman energy due to the internal field is much smaller than the Fermi energy: the difference between the up- and down-spin Fermi surface cross sections is only $\sim$2%, It is much lower than the resolution of the AMRO measurements.

B. Weakly incoherent transport and magnetoresistance

In the picture of the weakly incoherent interlayer transport, the interlayer transport between the adjacent layers is described as quantum tunneling.[25] Because of the stacking structure of layers I and II, the magnetic insulating layer (layer I) is recognized as a tunnel barrier for the interlayer transport. In zero magnetic field, the localized spins in layer I are randomly oriented. The antiferromagnetic spin fluctuation is enhanced below 20 K,[16] It suggests that the tunneling probability is reduced at low temperatures because of the random magnetic potential characterized by JS. The upturn of the resistance at zero field below 25 K in Fig. 2 is explained by the enhancement of the spin fluctuation. In strong magnetic field, the localized spins are more polarized and the fluctuation is suppressed, which makes the magnetic potential more homogeneous. It causes high tunneling probability (low resistance). The monotonic negative magnetoresistance under a field perpendicular to the layers (Figs. 5 and 8) is interpreted by the above magnetic potential effect. The saturation tendency of the negative magnetoresistance above 10 T likely corresponds to the saturation of the localized spin polarization.

Next, we consider the effect of the parallel field on the interlayer transport. The tunneling conductance between two 2D electron gas (2DEG) layers in a magnetic field parallel to the layers has been studied theoretically[39] and experimentally.[40] We assume that each layer (xy plane) has an identical 2D Fermi surface. In zero field, since the electrons get no momentum shift in the tunneling between the layers, the tunneling of all the electrons on the Fermi surface is permitted. However, in a parallel field ($H \parallel y$), the electrons get a momentum shift $\Delta k_x = eHd/\hbar$ in the tunneling, where d is the layer spacing. Because of the requirement of the momentum and energy conservation, the tunneling of the electrons is permitted only at the points where the two Fermi surfaces overlap each other after getting the momentum shift. This reduces the conductance; the positive magnetoresistance is induced (Fig. 12). In (Me-3,5-DIP)$[Ni(dmit)_2]_2$, there exist two 2D Fermi surfaces of the up and down spins. Because of the spin conservation, only the tunneling between the

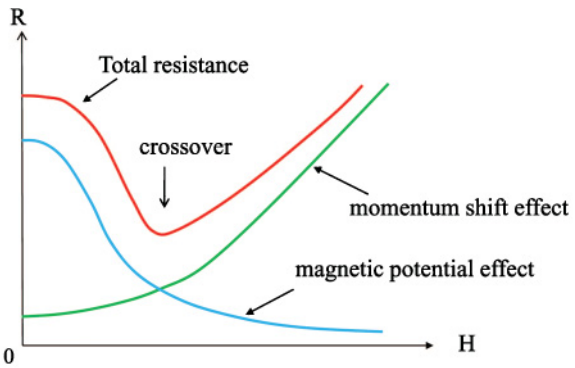

FIG. 12. (Color online) Schematic interpretation of the resistance minimum in parallel fields.

Fermi surfaces of the same spins is permitted. Therefore, the monotonic increase of the interlayer resistance with field is expected in (Me-3,5-DIP)[Ni(dmit)$_2$]$_2$. It is likely that the magnetic potential effect is dominant in low fields, but the effect of the momentum shifts in high fields. This would cause a resistance minimum (Fig. 12). The effect of the momentum shift is suppressed as the field is tilted from the layer direction to the perpendicular direction because the momentum shift Δk_x in the tunneling depends only on the field parallel to the layers. The sharp minimum and upturn of the resistance above 9 T is suppressed as θ decreases [Fig. 8(a)]. The behavior is consistent with the above picture. The sharp minimum at 9 T is evident at low temperatures [Fig. 8(b)]. It is also consistent with the NMR results, and the antiferromagnetic spin fluctuation is enhanced below 20 K.[16]

V. CONCLUSION

The organic conductor (Me-3,5-DIP)[Ni(dmit)$_2$]$_2$ has a 2D Fermi surface (itinerant electrons) in layer II and localized spins in layer I. The observed 2D Fermi surface is consistent with the band-structure calculation. Assuming an internal field of 13 T, arising from the exchange interaction between the spins in layers I and II, we can ascribe the two different frequencies of the quantum oscillations to the up- and down-spin Fermi surfaces. In a magnetic field parallel to the layers, the interlayer resistance has a minimum at ~8 T and shows the slow oscillation at higher fields. The resistance minimum at 8 T is interpreted as the crossover from the negative magnetoresistance due to the magnetic potential effect in the low-field region to the positive magnetoresistance due to the momentum shift effect in the high-field region. The origin of the slow oscillation in the high field is an open question.

ACKNOWLEDGMENTS

K.H. acknowledges support from the National Institute for Materials Science. This research was partially supported by a Grant-in-Aid for Scientific Research on Innovative Areas (No. 20110004) and Grant-in-Aid for Scientific Research (S) (No. 22224006) from the Japan Society for the Promotion of Science (JSPS).

[1] E. Coronado, J. R. Galan-Mascaros, C. J. Gomez-Garcia, and V. Laukhin, Nature (London) **408**, 447 (2000).
[2] N. Hanasaki, M. Matsuda, H. Tajima, T. Naito, and T. Inabe, J. Phys. Soc. Jpn. **72**, 3226 (2003).
[3] T. Konoike, S. Uji, T. Terashima, M. Nishimura, S. Yasuzuka, K. Enomoto, H. Fujiwara, B. Zhang, and H. Kobayashi, Phys. Rev. B **70**, 094514 (2004).
[4] S. Uji, H. Shinagawa, T. Terashima, T. Yakabe, T. Terai, M. Tokumoto, A. Kobayashi, H. Tanaka, and H. Kobayashi, Nature (London) **410**, 908 (2001).
[5] L. Balicas, J. S. Brooks, K. Storr, S. Uji, M. Tokumoto, H. Tanaka, H. Kobayashi, A. Kobayashi, V. Barzykin, and L. P. Gorkov, Phys. Rev. Lett. **87**, 067002 (2001).
[6] S. Uji and J. S. Brooks, J. Phys. Soc. Jpn. **75**, 051014 (2006).
[7] E. Coronad and P. Day, Chem. Rev. **104**, 5419 (2004).
[8] T. Enoki and A. Miyazaki, Chem. Rev. **104**, 5449 (2004).
[9] T. Inabe and H. Tajima, Chem. Rev. **104**, 5503 (2004).
[10] H. Kobayashi, H. Cui, and A. Kobayashi, Chem. Rev. **104**, 5265 (2004).
[11] J. Yamada, H. Akutsu, H. Nishikawa, and K. Kikuchi, Chem. Rev. **104**, 5057 (2004).
[12] T. Hayashi, X.-W. Xiao, H. Fujiwara, T. Sugimoto, H. Nakazumi, S. Noguchi, T. Fujimoto, S. Yasuzuka, H. Yoshino, K. Murata, T. Mori, and H. Aruga-Katori, J. Am. Chem. Soc. **128**, 11746 (2006).
[13] X.-W. Xiao, T. Hayashi, H. Fujiwara, T. Sugimoto, S. Noguchi, Y. Weng, H. Yoshino, K. Murata, and H. Aruga-Katori, J. Am. Chem. Soc. **129**, 12618 (2007).
[14] T. Sugimoto, H. Fujiwara, S. Noguchi, and K. Murata, Sci. Technol. Adv. Mater. **10**, 024302 (2009).
[15] Y. Kosaka, H. M. Yamamoto, A. Nakao, M. Tamura, and R. Kato, J. Am. Chem. Soc. **129**, 3054 (2007).
[16] S. Fujiyama, A. Shitade, K. Kanoda, Y. Kosaka, H. M. Yamamoto, and R. Kato, Phys. Rev. B **77**, 060403 (2008).
[17] C. Rossel, P. Bauer, D. Zech, J. Hofer, M. Willemin, and H. Keller, J. Appl. Phys. **79**, 8166 (1996); E. Ohmichi and T. Osada, Rev. Sci. Instrum. **73**, 3022 (2002).
[18] Y. Kosaka, Doctoral thesis, Saitama University, 2008.
[19] R. Yagi, Y. Iye, T. Osada, and S. Kagoshima, J. Phys. Soc. Jpn. **59**, 3069 (1990).
[20] Y. Iye, R. Yagi, N. Hanasaki, S. Kagoshima, H. Mori, H. Fujimoto, and G. Saito, J. Phys. Soc. Jpn. **63**, 674 (1994).
[21] J. Singleton, Rep. Prog. Phys. **63**, 1111 (2000).
[22] M. Kartsovnik, Chem. Rev. **104**, 5737 (2004).
[23] S. Uji, T. Terashima, S. Yasuzuka, J. Yamaura, H. M. Yamamoto, and R. Kato, Phys. Rev. B **68**, 064420 (2003).
[24] A. A. House, N. Harrison, S. J. Blundell, I. Deckers, J. Singleton, F. Herlach, W. Hayes, J. A. A. J. Perenboom, M. Kurmoo, and P. Day, Phys. Rev. B **53**, 9127 (1996).
[25] R. H. McKenzie and P. Moses, Phys. Rev. Lett. **81**, 4492 (1998); P. Moses and R. H. McKenzie, Phys. Rev. B **60**, 7998 (1999).
[26] J. Singleton, P. A. Goddard, A. Ardavan, N. Harrison, S. J. Blundell, J. A. Schlueter, and A. M. Kini, Phys. Rev. Lett. **88**, 037001 (2002).
[27] J. Wosnitza, J. Hagel, J. S. Qualls, J. S. Brooks, E. Balthes, D. Schweitzer, J. A. Schlueter, U. Geiser, J. Mohtasham, R. W. Winter, and G. L. Gard, Phys. Rev. B **65**, 180506 (2002).
[28] N. Hanasaki, S. Kagoshima, T. Hasegawa, T. Osada, and N. Miura, Phys. Rev. B **57**, 1336 (1998).
[29] T. Terashima, S. Uji, H. Aoki, M. Tamura, M. Kinoshita, and M. Tokumoto, Solid State Commun. **91**, 595 (1994).
[30] H. Tajima. S. Ikeda, M. Inokuchi, A. Kobayashi, T. Ohta, T. Sasaki, N. Toyota, R. Kato, H. Kobayashi, and H. Kuroda, Solid State Commun. **88**, 605 (1993).
[31] L. Balicas, J. S. Brooks, K. Storr, D. Graf, S. Uji, H. Shinagawa, E. Ojima, H. Fujiwara, H. Kobayashi, A. Kobayashi, and M. Tokumoto, Solid State Commun. **116**, 557 (2000).

[32]S. Uji, H. Shinagawa, Y. Terai, T. Yakabe, C. Terakura, T. Terashima, L. Balicas, J. S. Brooks, E. Ojima, H. Fujiwara, H. Kobayashi, A. Kobayashi, and M. Tokumoto, Physica B **298**, 557 (2001).

[33]T. Sasaki, H. Uozaki, S. Endo, and N. Toyota, Synth. Met. **120**, 759 (2001).

[34]D. Shoenberg, *Magnetic Oscillations in Metal*s (Cambridge University Press, Cambridge, UK, 1984).

[35]S. Uji, C. Terakura, T. Terashima, T. Yakabe, Y. Terai, M. Tokumoto, A. Kobayashi, F. Sakai, H. Tanaka, and H. Kobayashi, Phys. Rev. B **65**, 113101 (2002); S. Uji, H. Shinagawa, C. Terakura, T. Terashima, T. Yakabe, Y. Terai, M. Tokumoto, A. Kobayashi, H. Tanaka, and H. Kobayashi, *ibid*. **64**, 024531 (2001); S. Uji, T. Terashima, C. Terakura, T. Yakabe, Y. Terai, S. Yasuzuka, Y. Imanaka, M. Tokumoto, A. Kobayashi, F. Sakai, H. Tanaka, H. Kobayashi, L. Balicas, and J. S. Brooks, J. Phys. Soc. Jpn. B **72**, 369 (2003).

[36]K. Hiraki, H. Mayaffre, M. Horvatic, C. Berthier, S. Uji, T. Yamaguchi, H. Tanaka, A. Kobayashi, H. Kobayashi, and T. Takahashi, J. Phys. Soc. Jpn. **76**, 124708 (2007).

[37]T. Konoike, S. Uji, T. Terashima, M. Nishimura, S. Yasuzuka, K. Enomoto, H. Fujiwara, E. Fujiwara, B. Zhang, and H. Kobayashi, Phys. Rev. B **72**, 094517 (2005).

[38]S. Fujiyama, M. Takigawa, J. Kikuchi, H.-B. Cui, H. Fujiwara, and H. Kobayashi, Phys. Rev. Lett. **96**, 217001 (2006).

[39]J. P. Eisenstein, T. J. Gramila, L. N. Pfeiffer, and K. W. West, Phys. Rev. B **44**, 6511 (1991).

[40]J. A. Simmons, S. K. Lyo, J. F. Klem, M. E. Sherwin, and J. R. Wendt, Phys. Rev. B **47**, 15741 (1993).